7

SUMMARY AND CONCLUSION

7.1 SUMMARY

This study addressed the modelling of the effective thermal conductivity in a packed bed of mono-sized spheres. Although several accepted correlations for the effective thermal conductivity exist, these are based on porosity alone which does not fully account for the packing structure, especially in the near-wall region. Therefore, this study aimed to develop a new method of characterising the effective thermal conductivity, whilst accounting for the porous structure in a more fundamental manner (coordination number, contact angle).

In Chapter 1, the need to have a fundamental understanding of the impact of any wall region on not only porous structure, but also the effective thermal conductivity was identified. Previous studies suggested multiple constant correction factors in the wall region and the failure of existing models in the near-wall and wall regions.

Chapter 2 introduced various methods to represent the porous structure; with porosity the most widely used parameter. In addition to the literature reviewed, several parameters were developed for a randomly packed bed to help quantify the porous structure in such a way to be used for effective thermal conductivity calculations. This was achieved by using the coordinates of the positions of the spheres as generated by a DEM code. In addition, it was shown that the porous structure cannot be defined using porosity alone and that various characterisation methods (coordination number, contact angle, coordination flux number) should be used in conjunction with each other in order to successfully characterise the porous structure. The limitations on using porosity as the main parameter to quantify porous structure were also indicated.

Chapter 3 presented a summary of the effective thermal conductivity correlations found in literature. These correlations were grouped into three main components: heat transfer by point conduction, heat transfer by conduction through contact area and heat transfer by thermal radiation. It has been shown that relatively good accuracy can be obtained with several unit cell approaches in the bulk region of a packed bed, but that significant uncertainty arises in the near-wall and wall regions. A summary of all the correlations will be presented in Appendix A and Appendix B.

Chapter 4 presented a broad overview of the newly built HTTU. For the purpose of this study, experimental results conducted with the vacuum configuration to a temperature of 1200°C were used. The effective thermal conductivity results were extracted using a polynomial method and an uncertainty analysis was conducted in order to determine the confidence interval of the experimental results.

Chapter 5 presented the derivation of the Multi-sphere Unit Cell Model. This model was developed in such a way that it can be seen as a summary of all separate effects found for heat transfer in a porous structure of mono-sized spheres surrounded by a stagnant gas. This was achieved by using a thermal resistance network methodology for the conduction component and a radiative conductivity for the thermal radiation component. A clear distinction was made between the bulk and wall regions, for which separate heat transfer parameters were developed. In addition, a distinction was made between conduction through spheres with rough surfaces (rough contact network) and perfectly smooth surfaces (Hertzian contact network). Thermal radiation was grouped into two components: thermal radiation for spheres in contact (short-range radiation) and thermal radiation for spheres further apart (long-range radiation). Some uncertainty arose for the long-range radiation in the bulk, near-wall and wall regions for temperatures above 1200°C and materials with low conductivity.

Chapter 6 illustrated the validation and verification of the Multi-sphere Unit Cell Model and widely accepted existing correlations. It was shown that the Multi-sphere Unit Cell Model conduction component compares quite well with experimental data. For the SANA-I experimental test facility, the effective thermal conductivity measurements were extracted in a different manner to that used in past studies with effective thermal conductivity a function of radial position and not temperature. This illustrated the near-wall and wall effects more clearly. In addition, this highlighted the contribution of natural convection more clearly, showing two peaks near the inner and outer wall. Comparison between the Multi-sphere Unit Cell Model and the IAEA ZS Total correlation demonstrated the breakdown of the IAEA ZS model in the near-wall and wall region. For the HTTU experimental test facility, the Multi-sphere Unit Cell Model (total) and the IAEA ZS Total correlation demonstrated good comparison in the bulk region with experimental effective thermal conductivity values in both the 20 kW and 82.7 kW steady-states. However, the IAEA ZS Total correlation again demonstrated breakdown in the near-wall and wall regions where the Multi-sphere Unit Cell Model slightly under-predicted the experimental effective thermal conductivity results. A flowchart and summary of the Multi-sphere Unit Cell Model is presented in Figure 7.1 and Table 7.1.

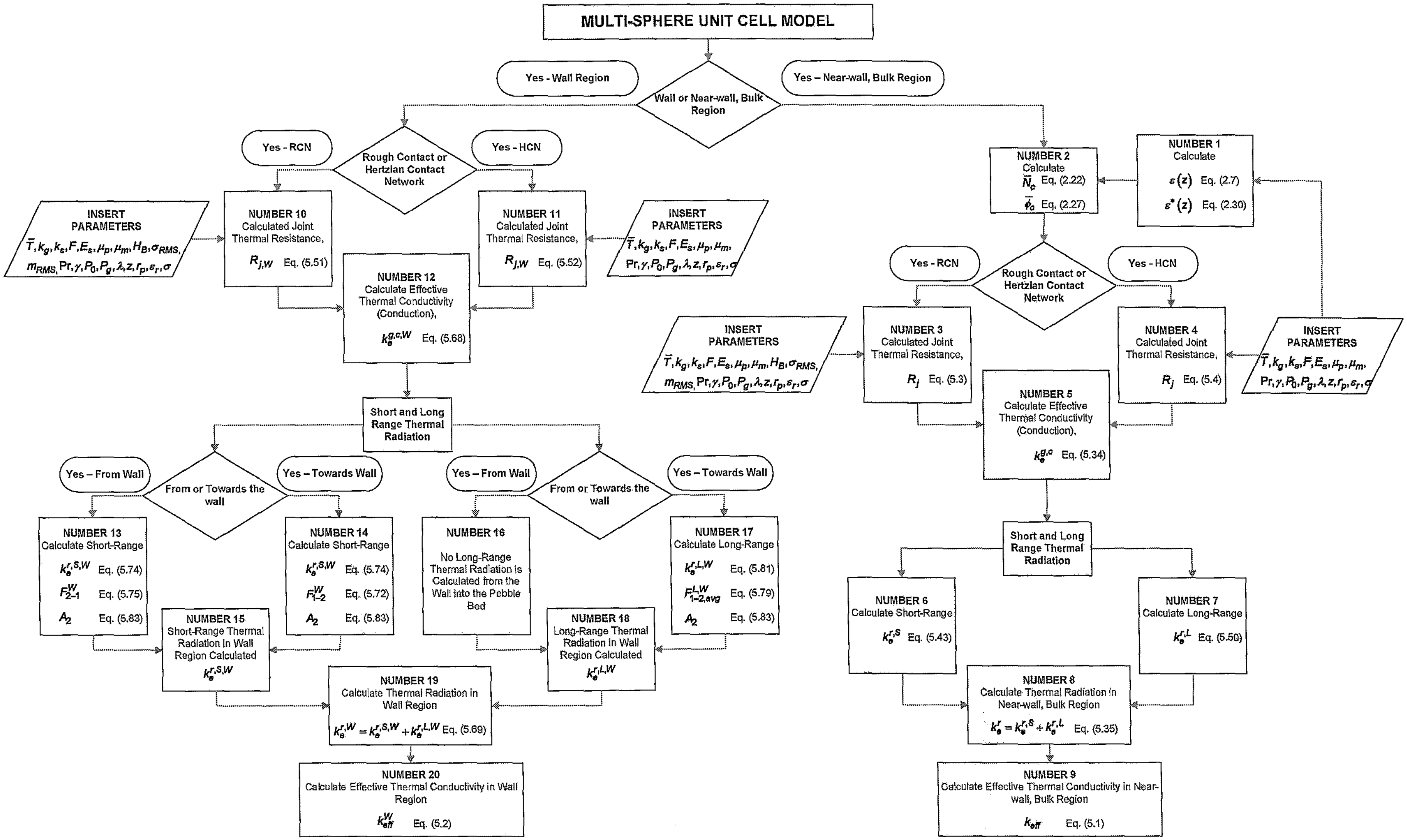

Figure 7.1: Flowchart of Multi-sphere Unit Cell Model

Table 7.1: Summary of Multi-sphere Unit Cell Model

BLOCK NUMBER	FORMULA	EQUATION NUMBER	BOUNDARY & ASSUMPTIONS	AUTHOR	COMMENTS
1	$\varepsilon(z)=2.14z^2-2.53z+1 \quad z\le 0.637$ $\varepsilon(z)=\varepsilon_b+0.29\exp(-0.6z)\times[\cos(2.3\pi(z-0.16))]+0.15\exp(-0.9z) \quad z>0.637$	(2.7)	Use when $z>3.8$ from wall.	De Klerk (2003:2022)	Calculation of radial porosity.
	$\varepsilon^*=-0.0127z^2+0.0967z-0.2011$	(2.30)	Use when $0.5<z\le 3.8$ in near-wall region.	*Derived in current study*	Calculation of porosity correction factor in near-wall region.
2	$\bar{N}_c=25.952\varepsilon^3-62.364\varepsilon^2+39.724\varepsilon-2.0233$	(2.22)	$(0.2398\le\varepsilon\le 0.54)$	*Derived in current study*	Calculation of average coordination number in a randomly packed bed.
	$\bar{\phi}_c=-6.1248\bar{N}_c^2+73.419\bar{N}_c-186.68$	(2.27)	$(0.2398\le\varepsilon\le 0.54)$	*Derived in current study*	Calculation of average contact angle in a randomly packed bed.
3	$R_j=\left(\frac{1}{R_{L,1,2}+\left(\frac{1}{R_g}+\frac{1}{R_s}\right)^{-1}}+\frac{1}{R_\lambda}+\frac{1}{R_G}\right)^{-1}+\left(\frac{1}{R_{in,1,2}}+\frac{1}{R_{mid,1,2}}+\frac{1}{R_{out,1,2}}\right)^{-1}$	(5.3)	—	*Derived in current study*	Calculation of joint thermal resistance with the Rough Contact Network (RCN) configuration.
	$R_s=\frac{0.565H^*\left(\frac{\sigma_{RMS}}{m_{RMS}}\right)}{k_sF}$	(3.105) (5.5)	$1.3\le H_B\le 7.6\ GPa$	Bahrami *et al.* (2006:3691)	Calculation of microcontact thermal resistance.
	$R_{L,1,2}=\frac{1}{2k_sr_a}$	(3.119) (5.6)	—	Bahrami *et al.* (2006:3691)	r_a is calculated with Eq. (3.113), contact area radius is renamed in the Multi-sphere Unit Cell Model as $r_a=a_L$

BLOCK NUMBER	FORMULA	EQUATION NUMBER	BOUNDARY & ASSUMPTIONS	AUTHOR	COMMENTS
3	$R_g = \frac{2\sqrt{2}\sigma_{RMS}a_2}{\pi k_g r_a^2 \ln\left(1+\frac{a_2}{a_1+\left(j/2\sqrt{2}\sigma_{RMS}\right)}\right)}$	(3.123) (5.7)	—	Bahrami *et al.* (2006:3691)	Calculation of the thermal resistance of the conduction through interstitial gas in contact region.
	$R_{in,1,2} = \frac{\left(d_p - \omega_0\right)}{k_s \pi r_a^2}$	(5.12)	—	*Derived in current study*	Calculation of the thermal resistance of the bulk solid material in the inner region, $\omega_0 = r_a^2 / 2r_{p,eq}$, $r_{p,eq} = r_p$.
	$R_\lambda = \frac{2}{\pi k_g \left(A_\lambda \ln\left\|\frac{A_\lambda - 2B_\lambda}{A_\lambda - 2C_\lambda}\right\| + 2B_\lambda - 2C_\lambda\right)}$	(5.22)	—	*Derived in current study*	Calculation of the thermal resistance of the interstitial gas in the middle region. $A_\lambda = 2r_p + j - \omega_0$, $B_\lambda = \sqrt{r_p^2 - r_\lambda^2}$, $C_\lambda = \sqrt{r_p^2 - r_a^2}$ and $r_\lambda = \sqrt{r_p^2 - \left(r_p - 0.5\omega_0 - 5\lambda\right)^2}$
	$R_{mid,1,2} = \frac{\left(d_p - \omega_0\right)}{k_s \pi \left(r_\lambda^2 - r_a^2\right)}$	(5.23)	—	*Derived in current study*	Calculation of the thermal resistance for the middle solid region.
	$R_G = \frac{2}{\pi k_g \left(A_G \ln\left\|\frac{A_G}{A_G - 2B_G}\right\| - 2B_G\right)}$	(5.27)	—	*Derived in current study*	Calculation of thermal resistance of the interstitial gas in the micro-gap. $A_G = 2r_p - \omega_0$, and $B_G = \sqrt{r_p^2 - r_\lambda^2}$
	$R_{out,1,2} = \frac{\ln\left\|\frac{A_{out} + B_{out}}{A_{out} - B_{out}}\right\|}{k_s \pi B_{out}}$	(5.32)	Assume isothermal temperature boundary.	*Derived in current study*	Calculation of the thermal resistance of the bulk solid material in the outer region. $A_{out} = r_p - 2\left(0.5\omega_0 + 5\lambda\right)$, $B_{out} = \sqrt{r_p^2 - r_\lambda^2}$

BLOCK NUMBER	FORMULA	EQUATION NUMBER	BOUNDARY & ASSUMPTIONS	AUTHOR	COMMENTS
4	$R_j = \left(\frac{1}{R_{HERTZ,1,2}} + \frac{1}{R_\lambda} + \frac{1}{R_G} \right)^{-1} + \left(\frac{1}{R_{in,1,2}} + \frac{1}{R_{mid,1,2}} + \frac{1}{R_{out,1,2}} \right)^{-1}$	(5.4)	—	*Derived in current study*	Calculation of joint thermal resistance with the Hertzian contact network configuration.
	$R_{HERTZ,1,2} = \frac{0.64}{k_s r_c}$	(5.8)	—	Chen & Tien (1973:302)	Hertzian contact radius r_c calculated by Eq. (3.101).
	$R_{in,1,2} = \frac{(d_p - \omega_0)}{k_s \pi r_c^2}$	(5.12)	—	*Derived in current study*	Calculation of the bulk solid material in the inner region, $\omega_0 = r_c^2 / 2r_p$.
	$R_\lambda = \frac{2}{\pi k_g \left(A_\lambda \ln \left\| \frac{A_\lambda - 2B_\lambda}{A_\lambda - 2C_\lambda} \right\| + 2B_\lambda - 2C_\lambda \right)}$	(5.22)	—	*Derived in current study*	Calculation of the thermal resistance of the interstitial gas in the middle region. $A_\lambda = 2r_p + j - \omega_0$, $B_\lambda = \sqrt{r_p^2 - r_\lambda^2}$, $C_\lambda = \sqrt{r_p^2 - r_c^2}$ and $r_\lambda = \sqrt{r_p^2 - (r_p - 0.5\omega_0 - 5\lambda)^2}$
	$R_{mid,1,2} = \frac{(d_p - \omega_0)}{k_s \pi (r_\lambda^2 - r_c^2)}$	(5.23)	—	*Derived in current study*	Calculation of the thermal resistance for the middle solid region.
	$R_G, R_{out,1,2}$	(5.27), (5.32)	—	*Derived in current study*	Same as given in block number 3.
5	$k_e^{g,c} = \frac{\bar{N}_c (d_p - \omega_0)}{2 d_p^2 R_j} \sin \bar{\phi}_c$	(5.34)	—	*Derived in current study*	Calculation of effective thermal conductivity (conduction component), ($\bar{\phi}_c$ is in degrees). $\omega_0 = r_a^2 / 2r_{p,eq}$ or $\omega_0 = r_c^2 / 2r_p$ depending on contact network used.

BLOCK NUMBER	FORMULA	EQUATION NUMBER	BOUNDARY & ASSUMPTIONS	AUTHOR	COMMENTS
6	$k_e^{r,S} = \dfrac{2\bar{N}_c d_p \sigma A_s \bar{T}^3}{A_r\left(\dfrac{2-2\varepsilon_r}{\varepsilon_r}+\dfrac{1}{F_{1-2}}\right)} f_k \sin\bar{\phi}_c$	(5.43)	$\Delta T/\bar{T} \ll 1$ $0.01 \le 1/\Lambda_s \le 10$ $0.2 \le \varepsilon_r \le 1$	*Derived in current study*	Calculation of short-range thermal radiation in the bulk and near-wall region. $F_{1-2} = 0.0756$, $A_s = 4\pi r_p^2$, $A_r = d_p^2$
7	$k_e^{r,L} = \dfrac{\bar{n}_{long} 5.32 d_p \sigma A_s \bar{T}^3}{A_r\left(\dfrac{2-2\varepsilon_r}{\varepsilon_r}+\dfrac{1}{F_{1-2,avg}^L}\right)} f_k$	(5.50)	$\Delta T/\bar{T} \ll 1$ for up to $2.25d_p$ $0.01 \le 1/\Lambda_s \le 10$ $0.2 \le \varepsilon_r \le 1$ f_k , $\bar{T}$ stays the same for thermal radiation between surfaces further apart than d_p .	*Derived in current study*	Calculation of long-range thermal radiation in the bulk and near-wall region. $F_{1-2,avg}^L = 0.0199$, $A_s = 4\pi r_p^2$, $A_r = d_p^2$ and $\bar{n}_{long} = 4.7$
8	$k_e^r = k_e^{r,S} + k_e^{r,L}$	(5.35)	$\bar{T} \le 1200°C$	*Derived in current study*	Summation of short and long-range thermal radiation.
9	$k_{eff} = k_e^{g,c} + k_e^r$	(5.1)	$\bar{T} \le 1200°C$	*Derived in current study*	Calculation of effective thermal conductivity due to thermal conduction and radiation in bulk and near-wall region. The limiting parameters for the Multi-sphere Unit Cell Model not reaching temperatures above 1200°C is: $1/\Lambda_s$ and the long-range radiation assumptions. The inverse of the dimensionless solid conductivity $1/\Lambda_s$ must be extended for lower conductivity solid materials. The long-range thermal radiation over estimates $k_e^{r,L}$ with $\bar{T} > 1200°C$.

BLOCK NUMBER	FORMULA	EQUATION NUMBER	BOUNDARY & ASSUMPTIONS	AUTHOR	COMMENTS
10	$R_{j,W}=\left(\dfrac{1}{R_{L,1,2}+\left(\dfrac{1}{R_g}+\dfrac{1}{R_s}\right)^{-1}}+\dfrac{1}{R_{\lambda,W}}+\dfrac{1}{R_{G,W}}\right)^{-1}+\left(\dfrac{1}{R_{in,1,W}}+\dfrac{1}{R_{mid,1,W}}+\dfrac{1}{R_{out,1,W}}\right)^{-1}$	(5.51)	—	*Derived in current study*	Calculation of joint thermal resistance with the Rough Contact Network (RCN) configuration in the wall region.
	$R_s=\dfrac{0.565H^*\left(\dfrac{\sigma_{RMS}}{m_{RMS}}\right)}{k_s^*F}$	(5.53)	$1.3\le H_B\le 7.6\ GPa$	Bahrami *et al.* (2006:3691)	Calculation of microcontact thermal resistance. $k_s^*=2k_{s1}k_{s2}/(k_{s1}+k_{s2})$
	$R_{L,1,2}=\dfrac{1}{2k_s^*r_a}$	(5.54)	—	Bahrami *et al.* (2006:3691)	r_a is calculated with Eq. (3.113), contact area radius is renamed in the Multi-sphere Unit Cell Model as $r_a=a_L$
	$R_g=\dfrac{2\sqrt{2}\sigma_{RMS}a_2}{\pi k_g r_a^2\ln\left(1+\dfrac{a_2}{a_1+\left(j/2\sqrt{2}\sigma_{RMS}\right)}\right)}$	(3.123) (5.7)	—	Bahrami *et al.* (2006:3691)	Calculation of conduction through interstitial gas in contact region.
	$R_{in,1,W}=\dfrac{(d_p-\omega_0)}{2k_s\pi r_a^2}$	(5.56)	—	*Derived in current study*	Calculation of the bulk solid material in the inner region, $\omega_0=r_a^2/2r_p$.
	$R_{\lambda,W}=\dfrac{1}{2\pi k_g\left(A_{\lambda,W}\ln\left\lvert\dfrac{B_{\lambda,W}-A_{\lambda,W}}{C_{\lambda,W}-A_{\lambda,W}}\right\rvert+B_{\lambda,W}-C_{\lambda,W}\right)}$	(5.61)	—	*Derived in current study*	Calculation of the thermal resistance of the interstitial gas in the middle region. $A_{\lambda,W}=r_p+j-\omega_0$, $B_{\lambda,W}=\sqrt{r_p^2-r_{\lambda,W}^2}$, $C_{\lambda,W}=\sqrt{r_p^2-r_a^2}$ and $r_{\lambda,W}=\sqrt{r_p^2-(r_p-\omega_0-10\lambda)^2}$

BLOCK NUMBER	FORMULA	EQUATION NUMBER	BOUNDARY & ASSUMPTIONS	AUTHOR	COMMENTS
10	$R_{mid,1}=\frac{(d_p-\omega_0)}{2k_s\pi\left(r_{\lambda,W}^2-r_a^2\right)}$	(5.62)	—	*Derived in current study*	Calculation of the thermal resistance for the middle solid region in the wall region.
	$R_{G,W}=\frac{1}{2\pi k_g\left(A_{G,W}\ln\left\|\frac{A_{G,W}}{B_{G,W}-A_{G,W}}\right\|-B_{G,W}\right)}$	(5.65)	—	*Derived in current study*	Calculation of thermal resistance of the interstitial gas in the micro-gap of the wall region. $A_{G,W}=r_p-\omega_0$ and $B_{G,W}=\sqrt{r_p^2-r_{\lambda,W}^2}$
	$R_{out,1,W}=\frac{\ln\left\|\frac{A_{out,W}+B_{out,W}}{A_{out,W}-B_{out,W}}\right\|}{2k_s\pi B_{out,W}}$	(5.66)	Assume isothermal temperature boundary.	*Derived in current study*	Calculation of the thermal resistance of the bulk solid material in the outer region of the wall region. $A_{out,W}=r_p-2(\omega_0+10\lambda)$ and $B_{out,W}=\sqrt{r_p^2-r_{\lambda,W}^2}$
11	$R_{j,W}=\left(\frac{1}{R_{HERTZ,1,2}}+\frac{1}{R_{\lambda,W}}+\frac{1}{R_{G,W}}\right)^{-1}+\left(\frac{1}{R_{in,1,W}}+\frac{1}{R_{mid,1,W}}+\frac{1}{R_{out,1,W}}\right)^{-1}$	(5.62)	—	*Derived in current study*	Calculation of joint thermal resistance with the Hertzian contact network configuration in the wall region.
	$R_{HERTZ,1,2}=\frac{0.64}{k_s^* r_c}$	(5.54)	—	Chen & Tien (1973:302)	Hertzian microcontact modified in this equation to accommodate k_s^*. Hertzian contact radius r_c calculated by Eq. (3.101).
	$R_{in,1,W}=\frac{(d_p-\omega_0)}{2k_s\pi r_c^2}$	(5.56)	—	*Derived in current study*	Calculation of the bulk solid material in the inner region, $\omega_0=r_c^2/2r_p$.
	$R_{\lambda,W}=\frac{1}{2\pi k_g\left(A_{\lambda,W}\ln\left\|\frac{B_{\lambda,W}-A_{\lambda,W}}{C_{\lambda,W}-A_{\lambda,W}}\right\|+B_{\lambda,W}-C_{\lambda,W}\right)}$	(5.61)	—	*Derived in current study*	Calculation of the thermal resistance of the interstitial gas in the middle region. $A_{\lambda,W}=r_p+j-\omega_0$, $B_{\lambda,W}=\sqrt{r_p^2-r_{\lambda,W}^2}$, $C_{\lambda,W}=\sqrt{r_p^2-r_c^2}$ and $r_{\lambda,W}=\sqrt{r_p^2-(r_p-\omega_0-10\lambda)^2}$

BLOCK NUMBER	FORMULA	EQUATION NUMBER	BOUNDARY & ASSUMPTIONS	AUTHOR	COMMENTS
11	$R_{mid,1} = \frac{(d_p - \varpi_0)}{2k_s\pi\left(r_{\lambda,W}^2 - r_c^2\right)}$	(5.62)	—	*Derived in current study*	Calculation of the thermal resistance for the middle solid region in the wall region.
	$R_{G,W}, R_{out,1,W}$	(5.65), (5.66)	—	*Derived in current study*	Same as given in block number 10.
12	$k_e^{g,c,W} = \frac{(r_p - \varpi_0)}{d_p^2 R_{j,W}}$	(5.68)	—	*Derived in current study*	Calculation of effective thermal conductivity in the wall region $\varpi_0 = r_c^2/2r_p$.
13	$k_e^{r,S,W} = \frac{2d_p\sigma\overline{T}^3}{A_r\left[\left(\frac{1-\varepsilon_{r,1}}{\varepsilon_{r,1}A_1}\right) + \frac{1}{A_1F_{1-2}^W} + \left(\frac{1-\varepsilon_{r,2}}{\varepsilon_{r,2}A_2}\right)\right]} f_k$	(5.74)	$\Delta T/\overline{T} << 1$ $0.01 \le 1/\Lambda_s \le 10$ $0.2 \le \varepsilon_r \le 1$	*Derived in current study*	Calculation of short-range thermal radiation in the wall region (Wall to Sphere). $F_{2-1}^W = 0.01976$, $A_r = d_p^2$, $A_1 = 4\pi r_p^2$ and $A_2 = 63.68\pi r_p^2$
14	$k_e^{r,S,W} = \frac{2d_p\sigma\overline{T}^3}{A_r\left[\left(\frac{1-\varepsilon_{r,1}}{\varepsilon_{r,1}A_1}\right) + \frac{1}{A_1F_{1-2}^W} + \left(\frac{1-\varepsilon_{r,2}}{\varepsilon_{r,2}A_2}\right)\right]} f_k$	(5.74)	$\Delta T/\overline{T} << 1$ $0.01 \le 1/\Lambda_s \le 10$ $0.2 \le \varepsilon_r \le 1$	*Derived in current study*	Calculation of short-range thermal radiation in the wall region (Sphere to Wall). $F_{1-2}^W = 0.315$, $A_r = d_p^2$, $A_1 = 4\pi r_p^2$ and $A_2 = 63.68\pi r_p^2$
17	$k_e^{r,L,W} = \frac{\overline{n}_{long}^W 4.536 d_p\sigma\overline{T}^3}{A_r\left[\left(\frac{1-\varepsilon_{r,1}}{\varepsilon_{r,1}A_1}\right) + \frac{1}{A_1F_{1-2,avg}^{L,W}} + \left(\frac{1-\varepsilon_{r,2}}{\varepsilon_{r,2}A_2}\right)\right]} f_k$	(5.81)	$\Delta T/\overline{T} << 1$ for up to $2.25d_p$ $0.01 \le 1/\Lambda_s \le 10$ $0.2 \le \varepsilon_r \le 1$ f_k , $\overline{T}$ stays the same for thermal radiation between surfaces further	*Derived in current study*	Calculation of long-range thermal radiation in the wall region. $F_{1-2,avg}^{L,W} = 0.02356$, $A_r = d_p^2$, $A_1 = 4\pi r_p^2$, $A_2 = 63.68\pi r_p^2$ and $\overline{n}_{long}^W = 1$

BLOCK NUMBER	FORMULA	EQUATION NUMBER	BOUNDARY & ASSUMPTIONS	AUTHOR	COMMENTS
			apart than d_p.		
19	$k_e^{r,W} = k_e^{r,S,W} + k_e^{r,L,W}$	(5.69)	$\bar{T} \leq 1200°C$	*Derived in current study*	Summation of short and long-range thermal radiation in wall region.
20	$k_{eff}^W = k_e^{g,c,W} + k_e^{r,W}$	(5.2)	$\bar{T} \leq 1200°C$	*Derived in current study*	Calculation of effective thermal conductivity due to thermal conduction and radiation in wall region. The limiting parameters for the Multi-sphere Unit Cell Model not reaching temperatures above $1200°C$ is: $1/\Lambda_s$ and the long-range radiation assumptions. The inverse of the dimensionless solid conductivity $1/\Lambda_s$ must be extended for lower conductivity solid materials. The long-range thermal radiation over estimates $k_e^{r,L}$ with $\bar{T} > 1200°C$.

7.2 CONCLUSION

It can thus be concluded that all the outcomes defined in Section 1.4 were met. Comprehensive research was conducted in order to understand and implement the various porous structure characterisation methods, and to develop a new empirical correlation relating the various methodologies. It was also demonstrated that the relation between porosity and coordination number is different in a randomly packed bed to what has been found in other studies. A new definition and method to calculate the effective thermal conductivity was presented that demonstrates relatively good agreement with the various experimental data sets. However, some additional research should be done expanding the Multi-sphere Unit Cell Model to calculate effective thermal conductivity beyond 1200°C and materials with low conductivity.

7.3 RECOMMENDATIONS FOR FURTHER RESEARCH

Recommendations can be made regarding further research with the objective of improving the Multi-sphere Unit Cell Model:

- Several shortcomings in experimental data sets can be identified in the relation to the development of a PBR:
  - Thermal conductivity tests should be conducted at low temperatures with graphite spheres. These tests need to be conducted using various applied forces and different surface roughness for different packings in the wall, near-wall and bulk regions. This is important because the surface roughness in a PBR changes with the constant bombarding of neutron flux. This research should also be conducted at vacuum and elevated pressures with helium as the gas medium.
  - Thermal radiation tests conducted at temperatures above 1200°C should also be conducted in the bulk, near-wall and wall regions. This is important because of the uncertainty that arose in effective thermal conductivity experiments above 1200°C in the HTO experimental test facility. This test should also be conducted at vacuum conditions and elevated pressure conditions with helium eliminating natural convection to an extent.
  - The impact on the effective thermal conductivity with the presence of a convex or concave curve should also be investigated at low and high temperatures. This is important because the HTTU could only achieve higher temperatures at the inner wall, where in general the outer wall and bulk regions should achieve equally high temperatures. CFD can possibly be used.

- Further research should also be conducted on the long-range radiation conductivity, for which the following areas are identified:
    - The long-range average diffuse view factor and average geometrical length needs to be derived as a function of radial position. Currently, the long-range average view factor is assumed to be the same in the bulk and near-wall regions, which is not the case in general.
    - The long-range average view factor must also be weighted according to the number of spheres that contribute to long-range thermal radiation.
    - The long-range average diffuse view factor in the wall region for thermal radiation heat transfer from a sphere to the wall should be investigated for a convex curved and a concave curved wall. Subsequently, the simulation answers need to be compared with relevant experimental data.
    - A new long-range non-isothermal correction factor needs to be derived using the same methodology applied for the derivation of the short-range non-isothermal correction factor.
    - The impact of the assumption that the average temperature between spheres not in contact is the same as that of the adjacent spheres should be further investigated.
- The non-isothermal correction factor Figure 5.11 should be extended $1/\Lambda_s > 100$ to accommodate thermal radiation between spheres with lower thermal conductivity.
- A constant emissivity for the HTTU was assumed and therefore the emissivity for the HTTU graphite needs to be obtained, in order to observe any impact it may have on simulation results. In addition the sphere conductivity should be obtained for the HTTU.
- The possibility of natural convection in the HTTU near-vacuum data should also be investigated, in order to clarify whether there is any increase in the effective thermal conductivity due to natural convective driven flows.

Lastly, it should be noted that the Multi-sphere Unit Cell Model can be used in collaboration with DEM codes, simulating the heat transfer between each and every pebble. This will enable a reduction in the degree of empiricism in simulating the porous structure. This means calculating temperatures in each pebble considering a stationary and a moving packed bed. The challenge lies in determining the heat flux vector through each pebble set in contact and correctly defining the long-range radiation parameter.